

# Effect of Lithium Ion Conduction on Hydrogen Desorption of $\text{LiNH}_2$ – $\text{LiH}$ Solid Composite

Tengfei Zhang,<sup>\*,†</sup> Shigehito Isobe,<sup>\*,†,‡</sup> Motoaki Matsuo,<sup>§</sup> Shin-ichi Orimo,<sup>||</sup> Yongming Wang,<sup>†</sup> Naoyuki Hashimoto,<sup>†</sup> and Somei Ohnuki<sup>†</sup>

<sup>†</sup>Graduate School of Engineering, Hokkaido University, N-13, W-8, Sapporo 060-8628, Japan

<sup>‡</sup>Creative Research Institution, Hokkaido University, N-21, W-10, Sapporo 001-0021, Japan

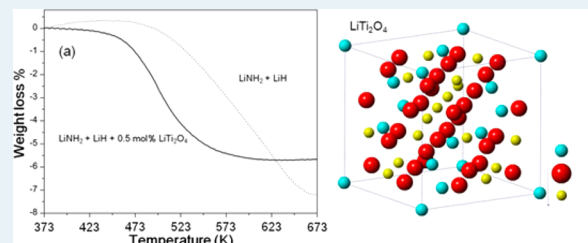
<sup>§</sup>Institute for Materials Research, Tohoku University, Sendai 980-8577, Japan

<sup>||</sup>WPI-Advanced Institute for Materials Research, Tohoku University, Sendai 980-8577, Japan

## S Supporting Information

**ABSTRACT:** This paper presents a relationship between ionic mobility and reaction kinetics for the Li–N–H system after doping  $\text{LiTi}_2\text{O}_4$ . The structural characteristic of this fast ionic conductor was introduced to the complex–hydride system. On one hand, the properties of the dehydrogenation process were improved significantly. On the other hand, the relationship between lithium ionic conductivity and the catalytic effect on the dehydrogenation was investigated according to the alternating current (AC) impedance results. The lithium ionic conductivity of samples with catalyst was higher than the samples without catalyst. Especially, the conductivity of  $\text{LiNH}_2$  and  $\text{LiH}$  mixtures with  $\text{LiTi}_2\text{O}_4$  was almost 1.5 times higher than that of  $\text{LiNH}_2$  and  $\text{LiH}$ . The mobility of the  $\text{Li}^+$  ions between  $\text{LiH}$  and  $\text{LiNH}_2$  solid phases was enhanced by adding  $\text{LiTi}_2\text{O}_4$ .

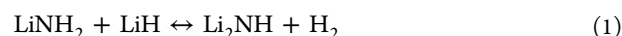
**KEYWORDS:** solid-state reactions, homogeneous catalysis, titanates, hydrogen storage, hydrides



Complex hydrides with the  $(\text{NH}_2)^-$  anion are generally expressed as  $\text{M}(\text{NH}_2)_n$  ( $n$ : valence of metal  $\text{M}$ ), which presents ionic bonding between the  $\text{M}^{n+}$  cation and the  $(\text{NH}_2)^-$  anion. Recently these materials have been researched actively as advanced hydrogen storage materials due to their high gravimetric and volumetric hydrogen densities.<sup>1–7</sup> Moreover, some of the researchers have reported that one of the complex hydrides,  $\text{LiNH}_2$ , expresses another chemical property, that is, lithium ionic conductivity.<sup>8–11</sup>

The study of lithium ionic conductivity is significantly important for two reasons. First, it may potentially be applied to the hydrogen fuel cell to improve the slow desorption kinetics and undesirable byproduct gases (such as ammonia). Second, it could be widely used in solid electrolytes to improve the safety and energy-density-related issues of lithium-ion batteries.<sup>10</sup>

The Li–N–H system has been consistently investigated with respect to its reversible reaction characteristics and relatively high  $\text{H}_2$  storage capacity since the first time it was reported in 2002.<sup>12</sup> The results of this previous investigation showed that hydrogen can be desorbed via the following reaction:



A large amount (6.5 wt %) of hydrogen is accessible in theory. However, the system is still limited for practical applications due to slow reaction kinetics and a high desorption temperature. It is worth noting that  $\text{NH}_3$  is a subsidiary product in the

dehydrogenation of the Li–N–H system according to eq 2. The main reason is because  $\text{LiNH}_2$  could decompose at higher temperatures.



Oxide–electrolyte materials with a special structure, such as spinels, perovskites, and fluorites, have been investigated actively with respect to the character of mobile interstitial ions and/or vacancies. Considering of the solid-state-reaction of complex hydrides, the mobile species of cations or anions also play an important role in the improvement of kinetics. Therefore, it is of reasonable interest to draw significance from the well-established oxide–electrolyte systems and provide the structural characteristics of these faster ionic materials to the complex hydride systems in order to accelerate the reaction kinetics.

At the same time, some authors have proposed in their reports the reaction based on  $\text{Li}^+$  migration across reactive interfaces between the  $\text{LiH}$  particles and the  $\text{LiNH}_2$  particles in eq 1.<sup>13–15</sup> On the basis of these results, we report another feasibility study of adding  $\text{LiTi}_2\text{O}_4$  as catalyst in the Li–N–H system, which shows better desorption kinetics and a purer product gas because of the increasing lithium ion conduction.

Received: August 22, 2014

Revised: February 5, 2015

Published: February 5, 2015

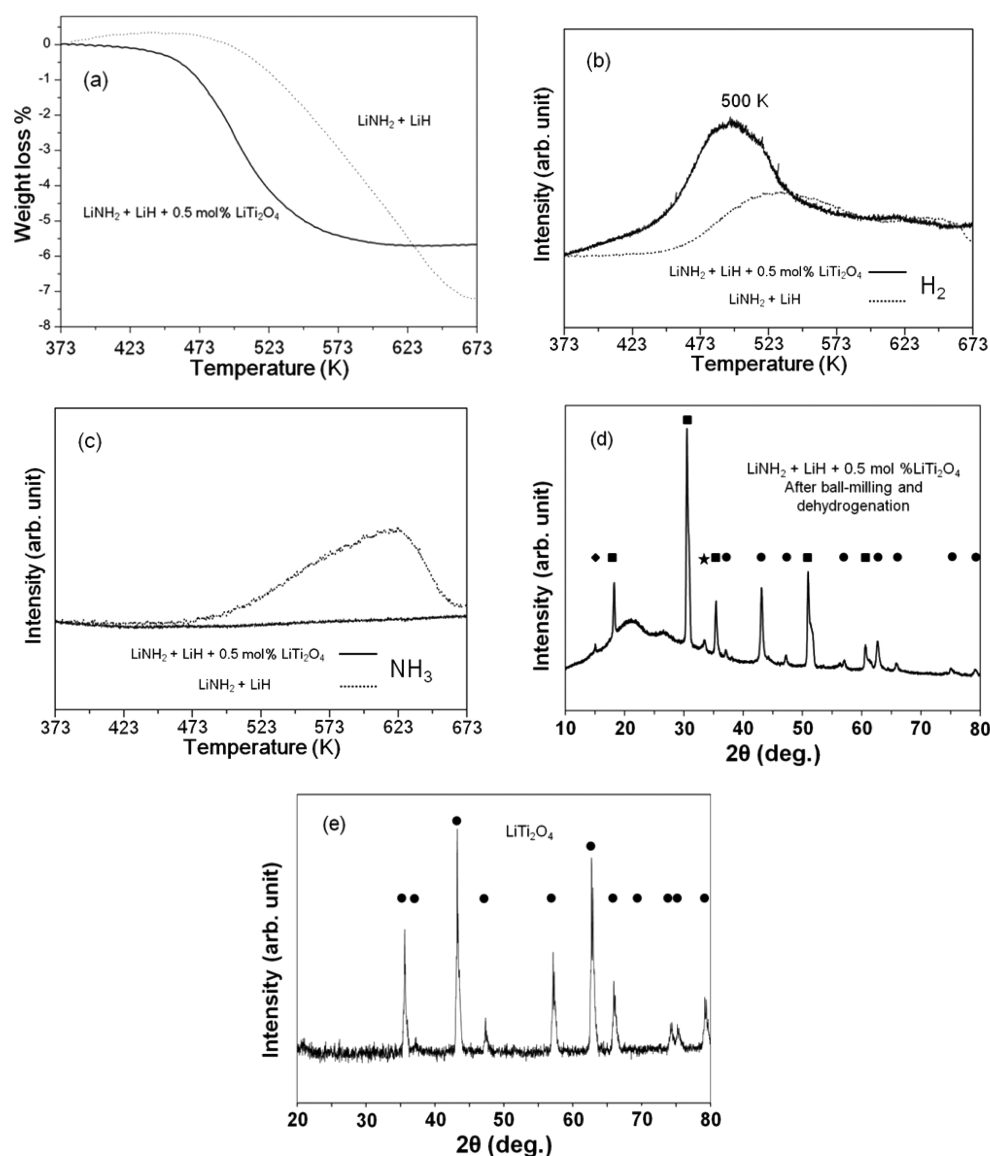


**Figure 1.** (a) Weight loss for the dehydrogenation of  $\text{LiNH}_2 + \text{LiH}$  mixture without any additive (dotted line) and with 0.5 mol %  $\text{LiTi}_2\text{O}_4$  (solid line); (b) Mass spectra of  $\text{H}_2$  gas desorption; (c) Mass spectra of  $\text{NH}_3$  gas desorption; (d) XRD pattern of the samples after high-energy ball milling and dehydrogenation; (e) XRD pattern of the single phase of  $\text{LiTi}_2\text{O}_4$ . ●:  $\text{LiTi}_2\text{O}_4$  (PDF 86-0631); ★:  $\text{Li}_2\text{O}$  (PDF 77-2144); ■:  $\text{Li}_2\text{NH}$  (PDF 06-0417); ◆:  $\text{LiOH}$  (PDF 32-564).

This study not only demonstrates an important direction to search for the reaction mechanism in complex hydrides but also introduces a novel way to target the catalyst in a solid-state reaction.

Experimental details are given in the Supporting Information. Concisely, the single phase of  $\text{LiTi}_2\text{O}_4$  was synthesized by a two-step solid-state reaction. In order to ensure a homogeneous mixing between the starting materials and the additive, ball-milling equipment was used. All the samples were measured by an ac impedance method to get the results of ionic conductivity. Temperature ranges for the conductivity measurements were set from room temperature to around 430 K.

The catalytic effect of  $\text{LiTi}_2\text{O}_4$  was indicated from the dehydrogenation process of the composite of  $\text{LiH}$  and  $\text{LiNH}_2$  with 0.5 mol %  $\text{LiTi}_2\text{O}_4$ . Figure 1a presented the thermogravimetry and differential thermal analysis (TG-DTA) results. During dehydrogenation, the mixture without additive was observed to start at 473 K and to complete at 673 K. In

contrast, a full desorption was exhibited from the sample with  $\text{LiTi}_2\text{O}_4$  within the temperature range of 383–583 K. The total weight loss for  $\text{LiNH}_2 + \text{LiH} + 0.5 \text{ mol } \% \text{ LiTi}_2\text{O}_4$  was 5.7 wt % compared with the 7.5 wt % for  $\text{LiNH}_2 + \text{LiH}$ .  $\text{NH}_3$ , which released from  $\text{LiNH}_2$  at high temperature, was the main reason for the different weight loss. This result of thermal gas desorption mass spectrometry is shown in Figure 1b,c. The sample with  $\text{LiTi}_2\text{O}_4$  addition exhibited a sharp  $\text{H}_2$  peak. The peak temperature was observed at 500 K. Ammonia was undetectable during the heating process. However, hydrogen and ammonia released from the sample without  $\text{LiTi}_2\text{O}_4$ . The broad hydrogen desorption curves and obvious ammonia emission can be seen from the beginning to the end of the reaction. The stability of  $\text{LiTi}_2\text{O}_4$  is reflected by the XRD patterns in Figure 1d. The structure of  $\text{LiTi}_2\text{O}_4$  was the same as the raw  $\text{LiTi}_2\text{O}_4$  after dehydrogenation (Figure 1e). The results demonstrated obviously that the purity of the desorbed hydrogen gas was improved after doping  $\text{LiTi}_2\text{O}_4$ . Accordingly,

a lower dehydrogenation temperature indicated that desorption properties can be improved greatly by adding  $\text{LiTi}_2\text{O}_4$  as the catalyst. Furthermore, the addition effect on hydrogen absorption of the mixture with  $\text{LiTi}_2\text{O}_4$  has been examined, which validated that the catalyst not only had an effect on dehydrogenation process but also on the hydrogenation process. These results were shown in the [Supporting Information](#).

In order to investigate the relationship between the catalytic effects and the ionic mobility, the electrical conductivities of the samples were measured by the ac impedance. It has been confirmed that the plot obtained using a lithium electrode exhibited only the semicircle, which is represented by a parallel combination of resistance and capacitance. Herein, one plot, which was obtained at 383 K, is shown in Figure 2a. Their

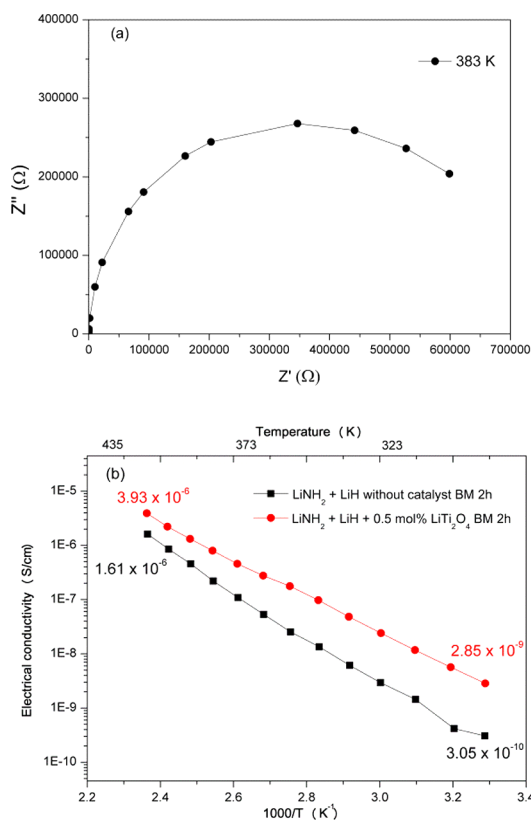


**Figure 2.** Electrical properties of samples with/without catalyst measured from RT to 423 K. (a) Typical impedance plots obtained using a lithium electrode at 383 K; (b) Arrhenius plots of the electrical conductivities for  $\text{LiNH}_2$  and  $\text{LiH}$  mixtures.

diameters decreased with increasing temperature. It was determined that the increased conductivity is due to the  $\text{LiNH}_2$  and  $\text{LiH}$  mixtures, not the metallic  $\text{LiTi}_2\text{O}_4$ . As shown in Figure 2b, the conductivity of  $\text{LiNH}_2$  and  $\text{LiH}$  with catalyst was  $3.93 \times 10^{-6}$  S/cm at 423 K, which was 1.5 times higher than the sample without catalyst following ball-milling at the same time. (In practice, the dwell time impedance measurement at each temperature is automatically determined for ensuring the accuracy and reproducibility and is usually between 90 and 120 min at each temperature. In this case, the mixture sample at 423 K consists of  $\text{LiNH}_2$ ,  $\text{LiH}$ , and  $\text{Li}_2\text{NH}$  with/without catalyst. The supplementary experiment is contained in the [Supporting Information](#).) The conductivity monotonically increased upon heating. Moreover, even though the ball-milling time had an

effect on lithium ionic conductivity, when the sample was subjected to ball-milling at the same time, the lithium ionic conductivities with 0.5 mol %  $\text{LiTi}_2\text{O}_4$  were higher than the sample without addition. The ionic conduction results of  $\text{LiTi}_2\text{O}_4$  respectively doping into  $\text{LiH}$  and  $\text{LiNH}_2$ , respectively, (as shown in the [Supporting Information](#)) as well as the mixture of them indicate that these Li compounds and their mixture inherently have lithium ionic conductivity, which is enhanced by  $\text{LiTi}_2\text{O}_4$  addition. The enhancement should be due to the improvement of  $\text{Li}^+$  mobility of the compounds rather than the increase of  $\text{Li}^+$  number from the additive  $\text{LiTi}_2\text{O}_4$  added only with 0.5 mol %.

In previous work,<sup>16</sup> it was usually assumed that the temperature dependence of the ionic conductivity can be expressed by an Arrhenius equation;

$$\sigma = A/T \exp(-E/kT)$$

where  $\sigma$  is the ionic conductivity,  $T$  is the absolute temperature,  $k$  is the Boltzmann constant,  $A$  is the pre-exponential factor, and  $E$  is the activation energy for conductivity. When  $\ln(\sigma T)$  is plotted against  $1/T$ , a straight line can be expected with a slope of  $-E/k$  and an intercept on the  $\ln(\sigma T)$  axis of  $\ln(A)$ . According to the results from Figure 2b, the temperature-dependent activation energy for conductivity of sample without and with catalyst can be deduced, 0.843 and 0.695 eV, respectively (Table 1). It can be seen that  $E$  decreases after adding catalyst. It is assumed that the lithium ion mobility is improved after adding catalyst.

**Table 1.** Correlation between  $E_a$  and  $E$  for Samples without and with Catalyst

sample	$E$ (activation energy of lithium conductivity, eV)	$E_a$ (activation energy of desorption, kJ/mol)
without catalyst	0.843	90.6
with catalyst	0.695	74.9

Furthermore, the activation energy of desorption ( $E_a$ ) was estimated by the Kissinger method<sup>17</sup> through measuring the mass spectra data at different heating rates, 6 K/min, 10 K/min, 14 K/min, and 18 K/min, separately, which is represented by the following equation.

$$\ln(\beta/T_p^2) = -E_a/RT_p + \ln(k_0R/E_a)$$

where  $\beta$  is the heating rate,  $T_p$  is the peak temperatures of desorption,  $R$  is the gas constant, and  $k_0$  is the frequency factor. If plotting  $\ln(\beta/T_p^2)$  as the function of the inverse of  $T_p$ , straight lines can be obtained, namely, the Kissinger plot. From the slope of the straight lines,  $E_a$  for the sample without and with catalyst was 90.6 kJ/mol  $\text{H}_2$  and 74.9 kJ/mol  $\text{H}_2$ , respectively (as shown in Table 1). It can be seen that  $E_a$  also decreases after doping catalyst. It is indicated that after doping catalyst, the reaction kinetics is improved due to the lithium ionic mobility increasing. It is clear that the increased conduction results in a lower hydrogen desorption temperature and an activation energy that is about 17% lower than the uncatalyzed sample.

These results suggest that, with the aid of the catalyst, the reaction kinetics can be enhanced, due to the increasing mobility of cations such as  $\text{Li}^+$  in compounds with special structure of catalyst. Herein, the details are given to explain the

reaction mechanism and the catalytic effect on the solid-state reaction between  $\text{LiNH}_2$  and  $\text{LiH}$ . For example, materials with fluorite structures are famous for their high conductivity.<sup>18</sup> Compared with the fast ionic fluorites,  $\text{LiNH}_2$  forms a similarly antifluorite structure, where the position of cations and anions are reversed. Therefore, it is unstable cations and  $\text{Li}^+$  which can migrate among different sites.<sup>19,20</sup> These results have been observed in the structure studies of  $\text{LiNH}_2/\text{Li}_2\text{NH}$ , which showed immigration of  $\text{Li}^+$  at high temperatures during dehydrogenation.<sup>13,15,21</sup> Additionally, our previous work has provided support for the reaction mechanism based on  $\text{Li}^+$  migration across reactive interfaces between  $\text{LiH}$  and  $\text{LiNH}_2$ .<sup>14</sup>

In the present studies,  $\text{LiTi}_2\text{O}_4$  has been experimentally proved to accelerate the lithium ionic conductivity to 1.5 times higher in the mixtures. The catalytic mechanism should be related to the crystal structure of  $\text{LiTi}_2\text{O}_4$ .  $\text{LiTi}_2\text{O}_4$  has a spinel-structure, where  $\text{Li}^+$  ions could go through into/out  $\text{LiTi}_2\text{O}_4$  without high energy barriers at ambient temperature.<sup>4,22</sup> Because of these characteristics of crystal structure,  $\text{LiTi}_2\text{O}_4$  has a high diffusion rate of  $\text{Li}^+$  which is reported to be  $10^{-8}$   $\text{cm}^2/\text{sec}$ .<sup>23</sup> All of these characters could help enhance the  $\text{Li}^+$  ions mobility in the  $\text{Li-N-H}$  system. Additionally, due to the complexity of solid-state reactions, it might be noted that besides the catalytic effect induced by this main mechanism, other effects of  $\text{LiTi}_2\text{O}_4$  on the mixing state before reacting, such as antisintering and enhanced homogeneous mixing of the reactants, probably also influence the reaction kinetics slightly.

We have reported the discovery of the relationship between the catalytic effect and the lithium ionic mobility. The conductivity of  $\text{LiNH}_2$  and  $\text{LiH}$  mixtures with catalyst is almost 1.5 times higher than the sample without catalyst, suggesting that the catalytic effect of  $\text{LiTi}_2\text{O}_4$  should mainly result from enhancing the mobility of the  $\text{Li}^+$  ions between the  $\text{LiH}$  and  $\text{LiNH}_2$  solid phases although it might probably involve other addition effects. We note that the structural characteristics of  $\text{LiTi}_2\text{O}_4$  could help improve the  $\text{Li}^+$  ionic mobility, which is the most critical factor in the phase transformation between Lithium amide and imide.<sup>12-15</sup> It is hoped that the  $\text{Li-N-H}$  system could be used not only in hydrogen storage but also in application of the lithium-ion battery materials.

## ■ ASSOCIATED CONTENT

### Supporting Information

The following file is available free of charge on the ACS Publications website at DOI: 10.1021/cs501782y.

Details of experimental procedures, data analysis methods and supporting experimental results ([PDF](#))

## ■ AUTHOR INFORMATION

### Corresponding Authors

\*E-mail: zhangtengfei@eng.hokudai.ac.jp.

\*E-mail: isobe@eng.hokudai.ac.jp.

### Notes

The authors declare no competing financial interest.

## ■ ACKNOWLEDGMENTS

This work was partially supported by L-station (Hokkaido University) and "Nanotechnology Platform" Program of the Ministry of Education, Culture, Sports, Science and Technology (MEXT), Japan.

## ■ REFERENCES

- (1) Züttel, A.; Borgschulte, A.; Orimo, S. *Scr. Mater.* **2007**, *56*, 823–828.
- (2) Orimo, S.; Nakamori, Y.; Eliseo, J. R.; Züttel, A.; Jensen, C. M. *Chem. Rev.* **2007**, *107*, 4111–4132.
- (3) Luo, W.; Sickafoose, S. *J. Alloys Compd.* **2006**, *407*, 274–281.
- (4) Zhang, T.; Isobe, S.; Wang, Y.; Hashimoto, N.; Ohnuki, S. *ChemCatChem.* **2014**, *6*, 724–727.
- (5) Chen, P.; Xiong, Z.; Luo, J.; Lin, J.; Tan, K. L. *J. Phys. Chem. B* **2003**, *107*, 10967–10970.
- (6) Zhang, T.; Isobe, S.; Wang, Y.; Oka, H.; Hashimoto, N.; Ohnuki, S. *J. Mater. Chem. A* **2014**, *2*, 4361–4365.
- (7) Aguey-Zinsou, K. F.; Yao, J.; Guo, Z. X. *J. Phys. Chem. B* **2007**, *111*, 12531–12536.
- (8) Anderson, P. A.; Chater, P. A.; Hewett, D. R.; Slater, P. R. *Faraday Discuss.* **2011**, *151*, 271–284.
- (9) Matsuo, M.; Sato, T.; Miura, Y.; Oguchi, H.; Zhou, Y.; Maekawa, H.; Takamura, H.; Orimo, S. *Chem. Mater.* **2010**, *22*, 2702–2704.
- (10) Matsuo, M.; Remhof, A.; Martelli, P.; Caputo, R.; Ernst, M.; Miura, Y.; Sato, T.; Oguchi, H.; Maekawa, H.; Takamura, H.; Borgschulte, A.; Züttel, A.; Orimo, S. *J. Am. Chem. Soc.* **2009**, *131*, 16389–16391.
- (11) Ohta, N.; Takada, K.; Zhang, L.; Ma, R.; Osada, M.; Sasaki, T. *Adv. Mater.* **2006**, *18*, 2226–2229.
- (12) Chen, P.; Xiong, Z.; Luo, J. Z.; Lin, J. Y.; Tan, K. L. *Nature* **2002**, *420*, 302–304.
- (13) (a) David, W. I. F.; Jones, M. O.; Gregory, D. H.; Jewell, C. M.; Johnson, S. R.; Walton, A.; Edwards, P. P. *J. Am. Chem. Soc.* **2007**, *129*, 1594–1601. (b) Makepeace, J. W.; Jones, M. O.; Callear, S. K.; Edwards, P. P.; David, W. I. F. *Phys. Chem. Chem. Phys.* **2014**, *16*, 4061–4070.
- (14) Zhang, T.; Isobe, S.; Wang, Y.; Hashimoto, N.; Ohnuki, S. *Rsc Adv.* **2013**, *3*, 6311–6314.
- (15) Cao, H.; Wang, J.; Chua, Y.; Wang, H.; Wu, G.; Xiong, Z.; Qiu, J.; Chen, P. *J. Phys. Chem. C* **2014**, *118*, 2344–2349.
- (16) Kilner, J. A.; Steele, B. C. H. In *Nonstoichiometric Oxides*; Sorensen, O. T., Ed.; Academic Press: New York, 1981; p 233.
- (17) Kissinger, H. E. *Anal. Chem.* **1957**, 1702–1706.
- (18) Conradi, M.; Corey, B.; Bowman, R.; Zidan, Jr., R. Stowe, A. private communication.
- (19) Allen, G. C.; Tempest, P. A.; Tyler, J. W. *Nature* **1982**, *295*, 48–49.
- (20) Wu, H. *ChemPhysChem* **2008**, *9*, 2157–2162.
- (21) Balogh, M. P.; Jones, C. Y.; Herbst, J. F.; Hector, L. G., Jr.; Kundrat, M. *J. Alloys Compd.* **2006**, *420*, 326–336.
- (22) Cava, R. J.; Murphy, D. W.; Zahurak, S. *J. Solid State Chem.* **1984**, *53*, 64–75.
- (23) Johnson, O. W. *Phys. Rev.* **1964**, *136*, A284–A290.